Applied Optics, 2005, Vol. 44, Issue 20, pp. 4360-4367

Performance of a photothermal detector with turbid liquids

Jane Hodgkinson [1,2,3], Mark Johnson [1,4] and John P Dakin[2]

1 North West Water Ltd, Dawson House, Warrington, WA3 3LW UK.

2 Optoelectronics Research Centre, University of Southampton, Southampton, SO17 1BJ UK.

3 Now at: Optical Sensors Group, School of Engineering, Cranfield University, Bedfordshire MK43 0AL UK. [address for correspondence]. email j.hodgkinson@cranfield .ac.uk

4 Now at: Instrumentation Design Ltd, Altrincham, WA14 4QN UK

Abstract

A closed-cell photothermal detector for aqueous analytes has been evaluated at 254nm and 678nm. The detector used a water meniscus as a pressure sensor, whose periodic deflection was measured using a low finesse optical fibre Fabry-Perot interferometer. Performance was compared with a commercial diode-array spectrometer and found to be similar for absorption measurements in non-turbid samples, but the results were affected up to 60 times less by scattered light. Finally the photothermal cell was converted into an integrating cavity using ceramic inserts, showing freedom from scattering related errors at 678nm but a degradation in performance at 254nm.

1 Introduction

The measurement of low absorption in the presence of strong light scattering remains an important challenge in environmental and biological analysis as well as the process industries. Photothermal (PT) and photoacoustic (PA) detection methods are therefore of interest because of their relative resistance to light scattering within the sample compared with conventional transmission spectrometers[1,2]. Typically, recent work on these techniques has involved the use of high power cw or pulsed lasers to give increased signal levels. Time resolution has enabled separation of the absorption and scattering related contributions to a

photoacoustic signal[3]. However, these systems are complex and the pulsed lasers they require are not always available at appropriate wavelengths at an acceptable cost.

Our approach has been to increase the sensitivity of a closed PT cell, such that signal levels are acceptable, even for low power, cw light sources such as laser diodes, UV discharge lamps and LEDs. A water meniscus has been used as a highly compliant pressure sensor at the top of a closed cell[4], with vertical movement of the centre of the meniscus detected using fibre optic interferometry.

There are relatively few reports that quantitatively compare the results of PA / PT detectors with more conventional methods of measuring optical absorption. Helander *et al* have investigated the effects of very high levels of light scattering internal to the sample[5], while McClelland and Knisely have discussed the effects of scattering from the sample to the cell wall[6], but without making any measurements on explicitly scattering bulk samples. Light scattering is expected to increase the measurement uncertainty for photothermal deflection spectroscopy and thermal lens spectroscopy, through a more spatially diffuse or attenuated measurement beam[7], though perhaps with better immunity to scattering than straightforward measurement of the transmitted light intensity[8].

We have now evaluated our detector with highly scattering water samples, whose turbidities spanned the range typically observed at water treatment intakes. The results were related to absorption coefficients using a coloured compound (potassium permanganate, $KMnO_4$) in aqueous solution. Our system has previously been demonstrated using a range of other wavelengths across the visible region[9]. To evaluate scattering effects we concentrated on our available wavelength extrema and compared performance to that of a commercial diode array spectrometer at 254nm and 678nm.

We further modified the cell, changing it from a transmission geometry to an integrating cavity. Integrating spheres have been previously used to make absorption measurements with good results[10,11], but there has been little work to combine the technique with PA methods[12]. The level of spurious signals resulting from side-wall absorption, in the manner of window noise[1], was uncertain.

2 Principle of operation

The photothermal system employed a flat water meniscus, constrained by surface forces, at a small (200 µm diameter) circular pinhole in nickel foil. Photothermal absorption of modulated light resulted in periodic pressure changes in the cell, which caused the meniscus to be deflected like a thin diaphragm, its curvature determined by the excess pressure in the cell. Zero dc pressure difference across the meniscus was maintained by a slow hydraulic leak to an outside reservoir, which equalised internal and external pressures on a timescale much longer than the modulation period in photothermal experiments. A schematic diagram of the apparatus is shown in Figure 1.

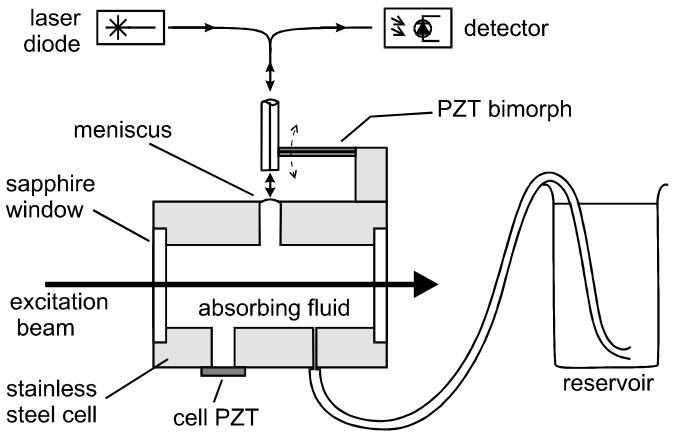

Figure 1. Schematic diagram of photothermal detector.

3 Theory of operation

The absorbed intensity I of a sample with an absorption coefficient α (in cm^{-1}) and optical pathlength L (in cm) is given by Beer's law. For turbid solutions, the additional use of a scattering coefficient s (in cm^{-1}) is well established[13], as follows;

$$I = I_0 \left\{ 1 - 10^{-(\alpha+s)L} \right\} \quad (1)$$

where I_o is the incident intensity. α and s are additive and may depend on wavelength.

For low frequency PT signal generation, we assume that all the absorbed light is instantly converted to heat. The deflection of the centre of the meniscus, Δh, has been shown to obey the following relationship[4].

$$\frac{\partial \Delta h}{\partial E} = \frac{\beta a^2}{4 C_p \rho \gamma} \frac{1}{\left(\frac{V_c}{\chi} + \frac{\pi a^4}{8\gamma} \right)} \quad (2)$$

E is the light energy absorbed by the fluid, β is the volume thermal expansion coefficient of the fluid, C_p is its specific heat capacity, ρ is its density, γ is its surface tension, χ is its bulk modulus, a is the radius of the meniscus (200μm), and V_c is the volume of fluid enclosed by the cell (1.6×10^{-5} m^3).

The use of low-finesse optical fibre interferometers for the measurement of small deflections is well established. The cleaved end of the interferometer fibre and the centre of the water meniscus together formed a low finesse Fabry-Perot cavity. Santos *et al* have analysed a similar cavity[14], and confirmed that for small reflectivities, an approximation to a two beam or Fizeau interferometer can be made, with multiple reflections at a low level. The interference fringes are then approximated by the following:

$$\phi = \phi_0 + A \cos\left(\frac{4\pi d}{\lambda} \right) \quad (3)$$

ϕ is the voltage signal from the detector (proportional to the detected fringe intensity), d is the distance separating the fibre end and the meniscus, λ is the interferometer wavelength, and A is a scale factor which is to be determined. At phase quadrature, the possible scale error resulting from the presence of multiple reflections is negligible[14] and the meniscus deflection may be calculated using the equation;

$$\delta d = \delta\phi \frac{\lambda}{4\pi A} \quad (4)$$

Self-referencing techniques have been used to improve the repeatability of the PT measurements[15]. These methods corrected for changes in the responsivity of the system, mainly due to interference fringe drift, (a change in the value of the scale factor A in equation (4)). A standard volumetric modulation was applied to the PT cell using a piezoelectric transducer ("cell PZT" in Figure 2), at a different frequency from the PT-excited signal. We took the ratio of (i) the photothermal signal from the analyte, to (ii) the self-referencing signal and converted this to a meniscus displacement Δh in nm, using the following calibration factor for an applied voltage of 9.48mVrms across the cell PZT;

$$\Delta h \quad = \quad (0.78 \pm 0.07)\text{nm} \ \frac{\text{PT signal}}{\text{PZT signal}} \qquad (5)$$

Following self referencing, it was estimated that the residual level of scale error on measured PT signals was up to ±9%, the precise error being dependent on environmental factors such as temperature stability.

4 Experimental details

Figure 2 shows the experimental apparatus, which has already been described in detail[4]. The entire apparatus was enclosed within an acoustic isolation chamber. The stainless steel PT cell had a pathlength of 5 cm and an internal diameter of 20 mm, with a highly polished inner surface. Sapphire windows were used for easy cleaning, and to minimise any possible PT window noise[1].

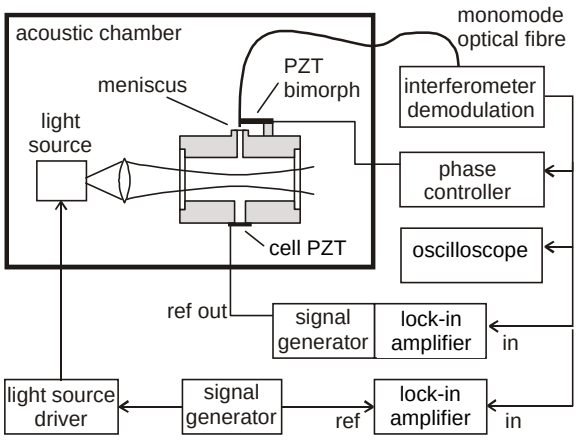

Figure 2. Experimental configuration for photothermal detection.

Two light sources were used for PT excitation experiments, chosen for their simplicity, low cost and high availability. The first source was a red laser diode module (RS 194-004) which could be square-wave modulated at frequencies above 100Hz. The second was a mercury discharge lamp (Spectronics Spectroline 11SC-1), driven via its proprietary driver (Spectroline SCT 1A/F), which was designed to run from a mains input. Variable frequency operation was achieved by connecting the signal generator output to a power amplifier (ILP SMOS 248), and using a transformer (RS 578-430) to provide the 240V required by the lamp driver. The lamp intensity was modulated as a rectified sine wave, the majority of the modulation

occurring at 2f. Stray light was reduced by covering the mercury tube with aluminium foil, apart from a 3mm hole from which light was coupled into the cell using a high NA lens.

Each light source was modulated at a frequency of 115Hz (=2f for the UV lamp). Using a calibrated photodiode, the modulated laser diode emission was estimated to be 1.4mWrms at 678nm, and the UV lamp output 0.3mWrms at 254nm, the emission wavelengths being confirmed by a diode array spectrometer (HP 8452A). The signal applied to the cell PZT, for self-referencing purposes, was 9.48mVrms at 90Hz. Cross-talk was confirmed to be negligible between the simultaneous signals from the PZT and those generated by either of the light sources.

The light sources were each driven by a Thurlby Thandar TG220 signal generator, and photothermal signals detected with an EG+G 5210 lock-in amplifier. The second lock-in amplifier was an EG+G 5110, which differed from the first only in its upper frequency limit. It drove the cell PZT though its internal signal generator, and detected the volumetric self-reference signal. Both lock-ins employed 100s integration periods. The cell PZT (Morgan Matroc PZT-5A) was a 0.45mm thick, 10mm square wafer, with electrodes on the two opposing faces, bonded to cover a 6mm diameter hole in the cell wall.

The optical fibre interferometer was used at phase quadrature, which was maintained by moving the end of the interferometer fibre with a piezoelectric bimorph element (RS 285-784), in a slow control loop with a time constant of approximately 0.2s. The distance between the cleaved optical fibre end and the centre of the meniscus was approximately 60-100 μm, which was much shorter than the coherence length of the 780nm laser diode used in the interferometer. This interferometer was then used to measure an rms noise floor for the meniscus displacement of 10 pm $Hz^{-1/2}$. Thus, with a 100s time constant, it was expected that deflections of 1pm would have a signal to noise ratio (SNR) of 1.

4.1 Preparation of samples

Experiments were performed on a range of concentrations of potassium permanganate ($KMnO_4$), and a range of suspensions of silica powder, both in deionised (DI) water. DI water was obtained from an Elgastat Option 4 deioniser[16] (stated to have specific resistance > 5 MΩ cm at 25°C, absorption by contaminants < 0.001AU at 254nm, 0.2 μm filtration used against particulates).

$KMnO_4$ is known to be a good standard for use as a photothermal absorber[17], because it doesn't fluoresce when excited in the visible, and delivers heat quickly to the solvent. Samples were made up by successive dilution from a stock solution containing a known quantity of the solid. No more than three serial dilutions were used, making the maximum estimated uncertainty in concentration less than 4% for the weakest solutions. $KMnO_4$ is known to be unstable in the presence of reducing agents. The sample absorptions were therefore checked before and after the experimental run and found to be stable to within the limits of the spectrometer, or to within ±3%, whichever was the higher.

Fused silica powder was used to create turbid solutions because of the known low level of optical absorption of pure silica at the wavelengths of interest, such that in the small quantities used here in water (3 – 500 ppm by weight) its effect on the background absorption would be negligible. The powder (P&R laboratories, ZZZ092018) had a quoted mean particle size of 3μm (information on its particle size distribution was not available). This mean size lies between that of the turbidity standard formazin (~6μm) and the submicron standards based on polymer spheres[18]. The turbidity of the suspensions in NTU (nephelometric turbidity units) was measured using a commercial turbidimeter (Hach 2100AN, filter no. 30312-00). The powder was observed to settle out over long time periods, so the containers were agitated to disperse the solid before samples were removed. Care was taken to take all comparative measurements (turbidimeter, spectrometer and photothermal detector) after the same length of subsequent settlement time (10-15 minutes). Any remaining settlement error was estimated to be below the specified accuracy of the instruments (±5% for the turbidimeter).

4.2 Experimental procedure

PT measurements were made as follows. The cell was rinsed with the solution to be tested, and then filled carefully, so as not to incorporate air bubbles. The interferometer fibre was roughly aligned to the centre of the meniscus, by eye, using an xyz stage. A sinusoidal voltage of approximately 10V peak-to-peak was applied to the cell PZT in order to modulate the height of the centre of the meniscus. The resulting fringes from the interferometer were displayed on an oscilloscope and used to align the fibre more precisely, to the position of maximum meniscus movement and to determine the correct quadrature setpoint for the phase controller. Measurements of PT-excited signals and the cell PZT-applied signals were used to determine the rms PT meniscus deflection as described in section 3.

For each of the samples used in the PT detector, comparative measurements were made using a diode array spectrometer (Hewlett Packard HP 8452A) with a 4cm pathlength silica cell, against a DI water blank.

5 Results

The absorption spectrum of a $KMnO_4$ solution and the scattering spectrum of a powdered silica suspension are shown in Figure 3.

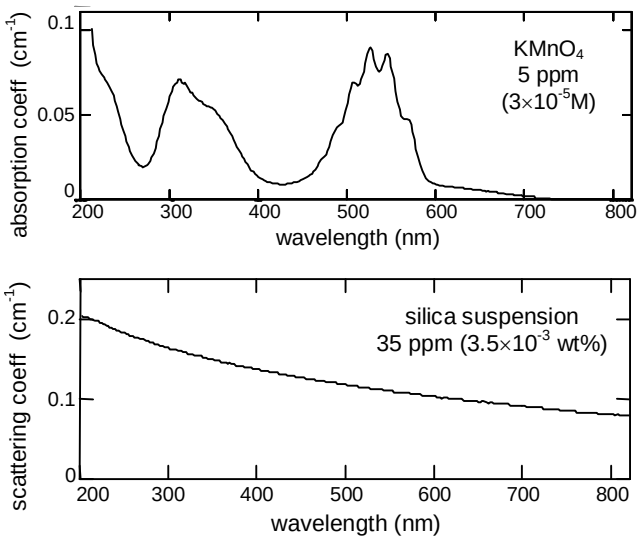

Figure 3. Absorption and scattering of $KMnO_4$ in aqueous solution and a suspension of silica powder, both taken with a diode array spectrometer using a 4cm cell, against a deionised water blank.

5.1 Light absorption by solutions of $KMnO_4$

The performance of the diode array spectrometer at 254nm and 678nm is shown in Figure 4. The absorption coefficient at both wavelengths was approximately $3\times10^{-4}cm^{-1}$ at a signal / noise ratio (SNR) of unity.

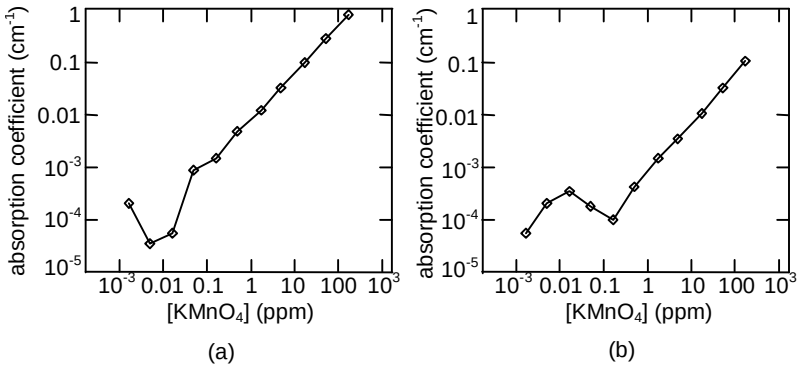

Figure 4. Absorption of aqueous solutions of $KMnO_4$, taken with a diode array spectrometer with a 4cm pathlength cell, against a deionised water blank. (a) 254nm, (b) 678nm.

The response of the PT system, in comparison, is shown in Figure 5 versus the measured rms meniscus deflection. As expected, the raw PT signals were proportional to the level of absorbed light, for high levels of absorption. At low levels of $KMnO_4$ they reached an asymptote determined by the absorption coefficient of water, taken here to be $17\times10^{-3}cm^{-1}$ at 254nm[19] and $4\times10^{-3}cm^{-1}$ at 678nm[19,20]. Subtraction of the signal for a deionised water blank shows the signal due to $KMnO_4$ alone, at low absorbances (Figure 5 (b)). We expect the instrument to be limited by an rms displacement noise of 1 pm as well as an estimated repeatability of up to ±9%, which is consistent with the absorption coefficient seen here for SNR=1, namely approximately $3\times10^{-4}cm^{-1}$ at 678nm and between $3\times10^{-3}cm^{-1}$ and $3\times10^{-4}cm^{-1}$ at 254nm.

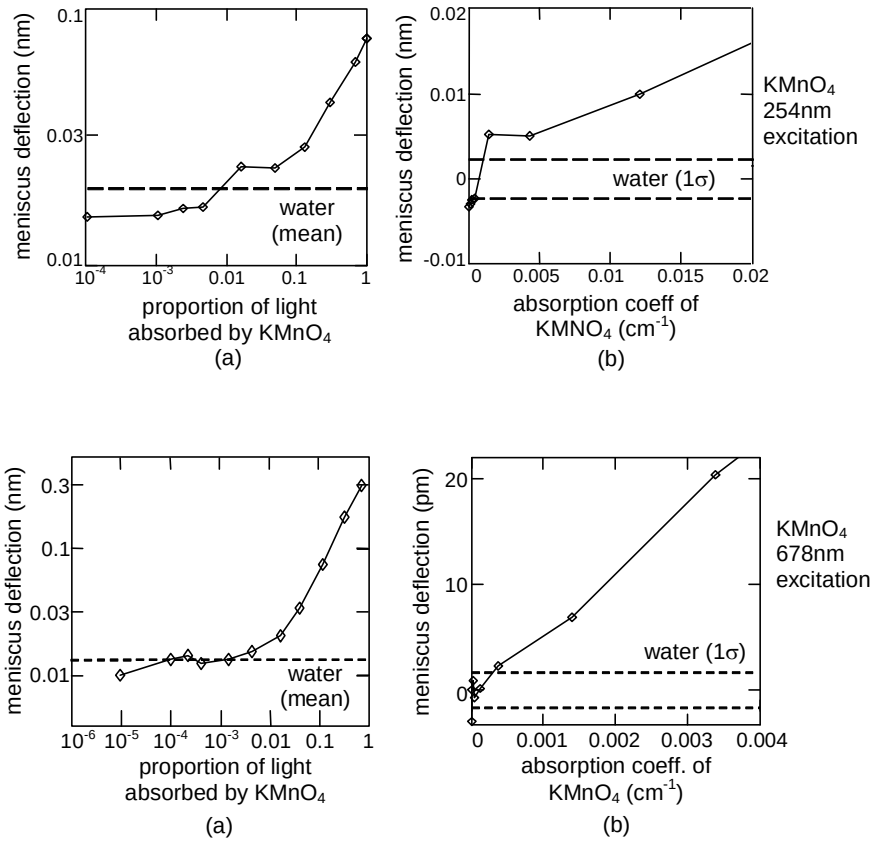

Figure 5. Photothermal signals resulting from absorption of light by $KMnO_4$ solutions from the UV lamp and the red laser diode. (a) Raw data. The dashed line shows the mean signal for a deionised water blank. (b) Following subtraction of the mean signal for deionised water (expanded scale). The dashed line shows one standard deviation in the signals for a deionised water blank.

Thus, the low α performance for the spectrometer and the photothermal detector appear similar when used to detect absorption over similar optical path lengths, in the absence of significant levels of light scattering.

5.2 Light scattering by suspensions of powdered silica

The performance of the diode array spectrometer in measuring each of the silica suspensions is shown in Figure 6 (a). The relationship between turbidity in NTU (measured with the turbidimeter) and the scattering coefficient *s* (measured with the diode array spectrometer) is expected to be broadly linear, since both

techniques use a similar optical method of measurement. Saturation can be seen at values of *s* approaching 1 cm^{-1}. At these high levels of turbidity, the "false positive" signal generated by the spectrometer is increased from the underlying absorption of water, by a factor of up to 53 (limited by apparent saturation) at 254nm and a factor of up to 225 at 678nm.

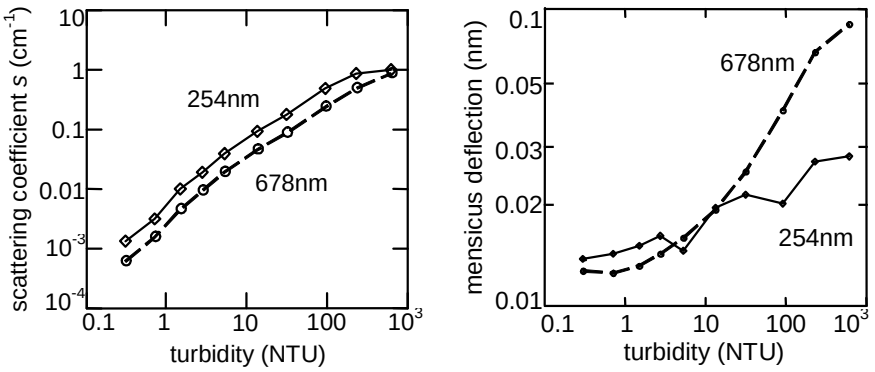

(a) (b)

Figure 6. Effect of turbidity on (a) the scattering coefficient *s*, measured using the diode array spectrometer, and (b) the magnitude of the photothermal signals.

PT signals recorded for the same silica suspensions, for light excitation at 254nm and 678nm, are shown in Figure 6(b). The low volume fractions of silica present were expected to have a negligible effect on the total absorption of the suspension, so at both wavelengths any change in the signal level should be due to light scattering alone.

Figure 7 shows the false-positive absorption coefficient resulting from light scattering, estimated by comparison with measurements made on deionised water controls. Figure 7(b) shows the improvement factor for the PT cell compared to the spectrometer. Although the errors have been magnified in this plot, especially at low levels of turbidity, it can be seen that the PT cell showed a significant improvement over the spectrometer, by up to a factor of 60 for the most highly scattering samples.

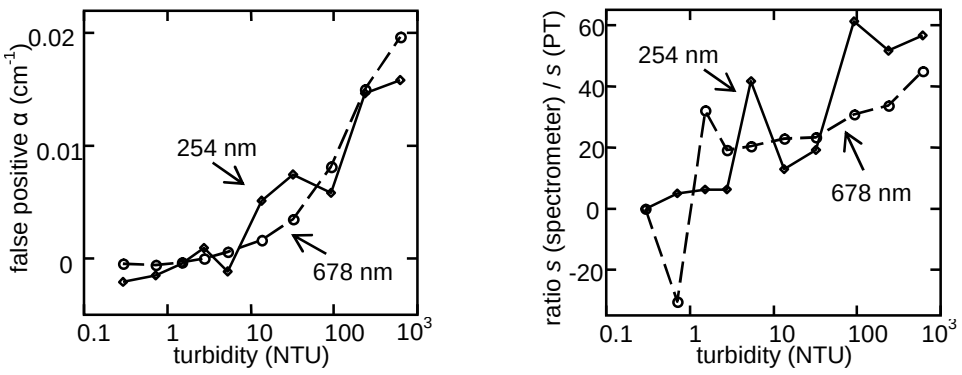

(a) (b)

Figure 7. (a) False-positive absorption results (or scattering coefficient) of turbid samples measured using a photothermal detector. (b) Ratio of scattering coefficient *s*, measured using the diode array spectrophotometer, to the false positive measurement made using the PT cell.

5.3 Use of a scattering insert to create an integrating cavity

To transform the PT cell into an integrating cavity, we used a thin (1mm) sleeve made from Macor, a white glass-ceramic (Corning Ltd) with high visible diffuse reflectivity and machinability[21] as well as low mechanical compliance., The sleeve was inserted into the cell and fitted snugly against the cell walls (Figure 8 shows the sleeve dimensions). Additional Macor endpieces were used adjacent to the sapphire windows (one containing an aperture just large enough to permit entry to the incoming light beam).

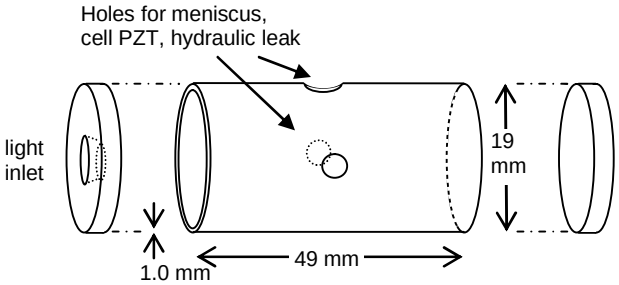

Figure 8. Macor sleeve insert and end pieces used to convert the cell into an integrating cavity.

Measurements were made with the integrating cavity style cell for both the absorbing solutions of $KMnO_4$ and the scattering suspensions of silica. The results shown in Figure 9 and Figure 10 can be compared with those in Figure 5 for the non-integrating cell. The integrating cavity appears to have increased the responsivity to $KMnO_4$ at 678nm by a factor of approximately two, and to have improved the minimum detectable absorption coefficient, both of which would be consistent with an increase in the effective pathlength. Unfortunately at 254nm the cell showed no response to additional absorption by $KMnO_4$, which suggests that absorption at the Macor cell wall may have given rise to large and dominant PT signals. The fact that meniscus deflections at this wavelength were so much greater than those recorded for the conventional PT cell is also consistent with this hypothesis.

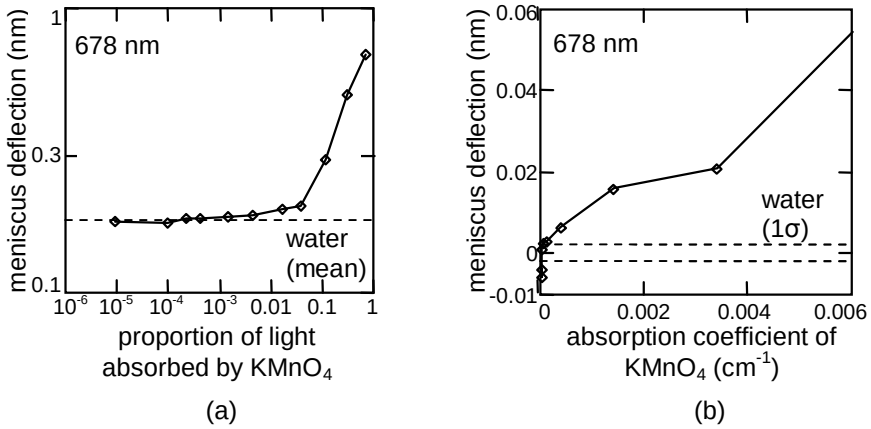

Figure 9. Photothermal signals resulting from absorption of light from the red laser diode by $KMnO_4$ solutions, inside the integrating cell. (a) Raw data. (b) Following subtraction of the mean signal for deionised water.

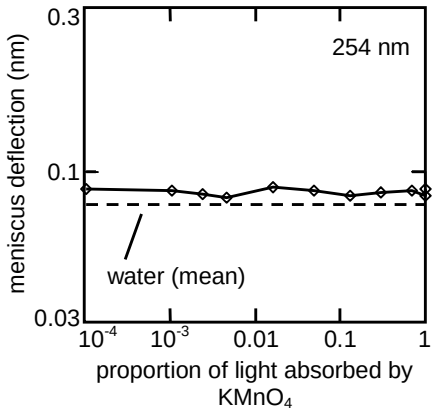

Figure 10. Photothermal signals resulting from absorption of UV light by $KMnO_4$ solutions, plotted on the same scale as Figure 9 for comparison. The results indicate a complete lack of sensitivity to additional UV absorption by $KMnO_4$, for the integrating cell.

Because of this lack of response to absorption at 254nm, any tolerance to turbidity at this excitation wavelength is of little interest. However, it can be seen in Figure 11 that at 678nm the new integrating cell showed remarkably little response to turbidity, any variation being at the level of measurement noise already established. Figure 12 quantifies the level of improvement in comparison with the results of section 5.2, showing minimal false positive absorption as a result of high turbidity, and improvement factors of up to 10^5 compared with a maximum factor of 45 observed previously at 678nm. (Since the false positive signals here essentially appear to be dominated by measurement noise rather than by any systematic effects of turbidity, their use as the denominator in such a ratio is not helpful, however the values have been included here for completeness.)

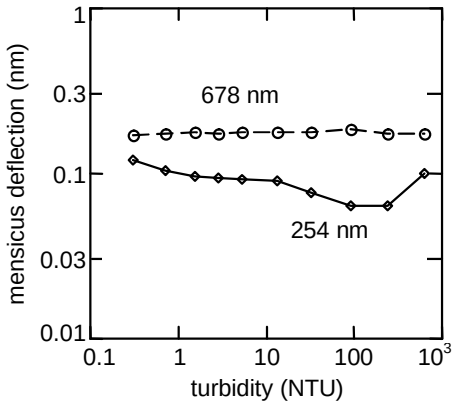

Figure 11. Effect of scattering on the magnitude of photothermal signals inside the integrating cavity

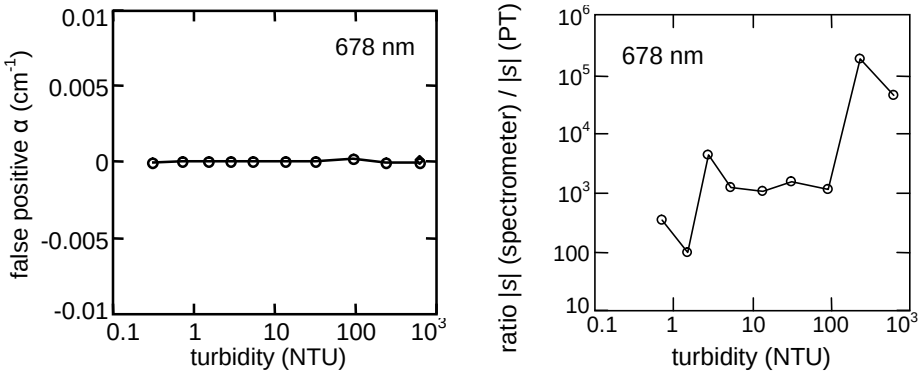

(a) (b)

Figure 12. Improvement in tolerance to analyte turbidity at 678nm using the integrating cavity. (a) False positive absorption coefficient (*s*) for turbid samples. (b) Ratio of the magnitude of false positive signals for the spectrometer, to the magnitude of the corresponding PT signals.

6 Discussion

In a conventional spectrometer, any scattered light is highly unlikely to reach the detector and so will be interpreted as absorption. In contrast, the acceptance aperture of a PA or PT detector is effectively larger, in that it can accommodate changes in the trajectories of light without generating such a large error.

The scattering coefficients recorded by the diode array spectrometer indicate that at the highest levels of turbidity in this study, the amount of incident light that passed right through the photothermal cell would have been minimal. There were therefore three more likely alternative outcomes for each photon entering the cell:

(i) Absorption at the side-walls, which would add to the photothermal signal because some of the heat generated by side-wall absorption could be transferred back into the fluid and cause it to expand[6].

(ii) Absorption by the fluid, with a potentially longer, convoluted pathlength[5].

(iii) Back-scattering out of the cell, reducing the signal if the mean interaction distance for backscattered photons were less than the length of the cell[5].

We can surmise that the change in PT signal due to effects (ii) and (iii) is likely to be small for the levels of scatter in our conventional PT cell. Any scattered rays having a significant additional, convoluted pathlength would be highly likely to strike the cell sidewall, giving rise to larger signals as discussed below.

The potential for increased signals caused by absorption of the incident beam at the side-walls of an ordinary transmission cell is considered greater for a long, thin cell, in which the scattered optical thickness (determined from Figure 6) is longer than the diameter of the cell. An estimate of the potential magnitude of this effect has been determined experimentally. The incident beams from the laser diode and the mercury lamp were directed straight towards the stainless steel side-wall, rather than through the centre of the cell, in a cell containing deionised water alone. The beams then exited the cell, having reflected once only, with an optical path length only 10% longer than would normally be the case. The resulting photothermal signals are summarised in Table 1, and compared to the measured signals from the most turbid silica suspension.

Table 1. RMS photothermal meniscus deflection for excitation in a highly turbid sample, and as a result of absorption at the cell side-wall (uncertainties estimated from residual scale errors following self-referencing)

Excitation wavelength	**Photothermal meniscus deflection**		
	deionised water (no scattering)	**610 NTU sample**	**Side-wall absorption experiment**
254nm	16±1.4 pm	33±3 pm	27±2 pm
678nm	15±1.4 pm	92±8 pm	63 ±6 pm

The results in Table 1 are of the same order of magnitude as our increased PT signals for turbid samples, suggesting that side-wall absorption could be sufficient to account for the increase. Although the effects of light scattering at 254nm are expected to be higher than those experienced at 678nm, Table 1 shows reduced absorption at the side-wall at 254nm, which could partially compensate.

For better resistance to light scattering, PT and PA cells that have a small aspect ratio (ie are short and fat) are likely to experience less side-wall absorption. Unfortunately, long, thin cells with a higher aspect ratio can offer greater PA or PT sensitivity in the absence of scattering, since the shape of the cell can be more closely matched to the shape of the light beam from well-collimated light sources, with a longer optical pathlength and less dead volume of fluid[22]. Thus, even for a PA or PT detector, there can be a trade-off between measurement sensitivity and resistance to light scattering.

The use of Macor to create an integrating cavity in our later experiments had two possible outcomes, as exemplified by our results at 254nm and 678nm. Clearly, any light entering the cell would either be absorbed by the fluid or the sidewall, or leave the cell via the entrance aperture. Having a small aperture could therefore have resulted in little opportunity for backscattered light to escape, as in (iii). A relatively high level of sidewall absorption compared to the fluid might then preclude any sensitivity to absorption changes within the fluid. At 254nm, we believe strong sidewall absorption and efficient heat transfer back into the fluid resulted in signals that dominated any PT measurements of absorption within the fluid. The PT cell was as insensitive to turbidity as it was to any change in absorption within the analyte.

At 678nm, an alternative outcome was observed, presumably because of much reduced levels of side-wall absorption. We believe the high level of scattering by the cell wall itself now dominated the light distribution, giving tolerance to light scattering that was at or below the measurement noise of $<2\times10^{-4}cm^{-1}$. The responsivity of the cell was increased and its minimum detectable absorption coefficient improved, both consistent with a longer effective pathlength. This success may have been due to a favourable balance between a low level of sidewall absorption excited signals and an appropriately sized aperture, neither of which have been specifically optimised.

7 Conclusion

The ability to detect trace contaminants in water, in the presence of turbidity, is of great importance. Our low frequency photothermal detector, which employs low power light sources, has been tested using a range of absorbing liquids and suspensions of light scatterers with turbidities in the range 0.3-600 NTU. A novel integrating cavity PT cell was also created using Macor machinable ceramic, within the geometrical confines of the original cell. A conventional diode array spectrometer was used for comparison.

The minimum detectable absorption coefficients of the PT detector and the spectrometer were similar. However, the PT technique was far less affected by light scattering than the spectrometer, giving false positive results that were reduced by up to a factor of 60 compared to the spectrometer. Turbidity is believed to increase the PT response by a possible combination of two mechanisms, (i) deflection of photons towards the cell walls, where they may be absorbed and give rise to a spurious signal, and (ii) increased average pathlengths. It was shown experimentally that the first effect could account for most, if not all, the increased signals in our most turbid solutions in the PT transmission cell.

A bigger improvement was observed in the integrating PT cell at 678nm, where responsivity was improved by a factor of two, the minimum detectable absorption coefficient was reduced, and the cell showed good tolerance to turbidity, at or below the measurement noise. However at 254nm the response was substantially degraded, probably caused by high levels of absorption by the sidewalls in the integrating cell. We conclude that PT / PA detection and their combination with integrating cavities of appropriate reflectivity show good promise for the analysis of turbid media, the choice of technique depending on the levels of turbidity and of sidewall absorption at the wavelengths of interest.

Acknowledgements

The authors are grateful for the support provided by North West Water Ltd and by the UK Department of Trade and Industry, through the Teaching Company Scheme.

References

1. A. Rosencwaig, *Photoacoustics and photoacoustic spectroscopy*. (Wiley, New York, 1980).

2, Y.-H. Pao, *Optoacoustic spectroscopy and detection.* (Academic Press, New York, 1977).

3 JR Small, NS Foster, JE Amonette and T Autrey, "Listening to colloidal silica particles: Simultaneous measurement of absorbed and scattered light using pulsed laser photoacoustics," Appl. Spectrosc. **54,** 1142-1150 (2000)

4. J. Hodgkinson, M. Johnson and J. P. Dakin, "Photoacoustic detection using the deflection of a water meniscus," Meas. Sci. Tech. **9**, 1316-1323 (1998)

5 P Helander, I Lundström and D McQueen, "Light scattering effects in photoacoustic spectroscopy," J. Appl. Phys. **51**, 3841-3847 (1980)

6 JF McClelland and RN Kniseley, "Photoacoustic spectroscopy with condensed samples", Appl. Opt. **15**, 2658-2663 (1976)

7 JD Spear, RE Russo and RJ Silva, "Collinear photothermal defection spectroscopy with light-scattering samples", Appl. Opt. **29,** 4225-4234 (1990)

8 JB Thorne and DR Bobbitt, "Comparison of Beer's law and thermal lens techniques for absorption measurements under conditions of high scattering backgrounds," Appl. Spectrosc. **47**, 360-363 (1993)

9 J Hodgkinson, M Johnson and JP Dakin. "Photothermal detection of trace optical absorption in water by use of visible-light-emitting diodes," Appl. Opt. **37** 7320-7326 (1998)

10 E S Fry, G W Kattawar and R M Pope, "Integrating cavity absorption meter," Appl. Opt. **31** (12), 2055-2065 (1992)

11 I Fecht and M Johnson, "Non-contact, scattering-independent water absorption measurement using a

falling stream and integrating sphere," Meas. Sci. Technol. **10**, 612-618 (1999)

12 A Yarai, Y Okamoto, and T Nakanishi, "High-sensitivity photothermal radiometry measurement using a mirrored liquid sample vessel for multireflection of a pumping beam," Rev. Sci. Instrum. **74** (1), 652-654 (2003)

13. G F Lothian and F P Chappell, "Transmission of light through suspensions," J. Appl. Chem. **1**, 475-482 (1951)

14 JL Santos, AP Leite and DA Jackson, "Optical fibre sensing with a low-finesse Fabry-Perot cavity," Appl. Opt. **31** (34), 7361-7366 (1992)

15. J Hodgkinson, M Johnson and J P Dakin, "Comparison of self-referencing techniques for photothermal detection of trace compounds in water," Sensor Actuat. B-Chem. **67,** 227-234 (2000)

16 Elgastat Option 4 water deioniser Operators Handbook. Elga Ltd, High Wycombe, UK (1994)

17. S. E. Braslavsky and G. E. Heibel, "Time-resolved photothermal and photoacoustic methods applied to photoinduced processes in solution," Chem. Rev. **92** 1381-1410 (1992)

18 K Papacosta, "Turbidity calibration standards evaluated from a different perspective," Proc. Federal Interagency Workshop on Turbidity and other Sediment Surrogates, Reno, NV, US Geological Survey Circular 1250 (2002)

19. G M Hale and M R Querry, "Optical constants of water in the 200-nm to 200-μm wavelength region," Appl. Opt. **12,** 555-563 (1973)

20. C K N Patel and A C Tam, "Pulsed optoacoustic spectroscopy of condensed matter" Rev. Mod. Phys. **53,** 517-550 (1981)

21 D S Goodman, "Machinable glass ceramic: a useful optical material," Appl. Opt. **25** (11), 1726-1726 (1986)

22 LG Rosengren, "Optimal optoacoustic detector design", Appl. Opt. **14**, 1960-1976 (1975)